ELSEVIER

Biochimica et Biophysica Acta 1506 (2001) 244–259

BIOCHIMICA ET BIOPHYSICA ACTA
BBA

www.bba-direct.com

Involvement of zeaxanthin and of the Cbr protein in the repair of photosystem II from photoinhibition in the green alga *Dunaliella salina*

EonSeon Jin, Juergen E.W. Polle, Anastasios Melis *

Department of Plant and Microbial Biology, 111 Koshland Hall, University of California, Berkeley, CA 94720-3102, USA

Received 11 July 2001; accepted 27 September 2001

Abstract

A light-sensitive and chlorophyll (Chl)-deficient mutant of the green alga *Dunaliella salina* (*dcd*1) showed an amplified response to irradiance stress compared to the wild-type. The mutant was yellow–green under low light (100 μmol photons m^{-2} s^{-1}) and yellow under high irradiance (2000 μmol photons m^{-2} s^{-1}). The mutant had lower levels of Chl, lower levels of light harvesting complex II, and a smaller Chl antenna size. The mutant contained proportionately greater amounts of photodamaged photosystem (PS) II reaction centers in its thylakoid membranes, suggesting a greater susceptibility to photoinhibition. This phenotype was more pronounced under high than low irradiance. The Cbr protein, known to accumulate when *D. salina* is exposed to irradiance stress, was pronouncedly expressed in the mutant even under low irradiance. This positively correlated with a higher zeaxanthin content in the mutant. Cbr protein accumulation, xanthophyll cycle de-epoxidation state, and fraction of photodamaged PSII reaction centers in the thylakoid membrane showed a linear dependence on the chloroplast 'photoinhibition index', suggesting a cause-and-effect relationship between photoinhibition, Cbr protein accumulation and xanthophyll cycle de-epoxidation state. These results raised the possibility of zeaxanthin and Cbr involvement in the PSII repair process through photoprotection of the partially disassembled, and presumably vulnerable, PSII core complexes from potentially irreversible photooxidative bleaching.

Keywords: Chlorophyll antenna size; Photoinhibition; Zeaxanthin; Cbr protein; Photosystem II repair; *Dunaliella salina*

1. Introduction

Plants and algae adjust the structure and function of the photosynthetic apparatus in response to change in their growth environment. Specifically, adjustments in pigment content and composition, and photosystem organization are important because they confer acclimation to the prevailing irradiance conditions [1,2]. Pigments such as chlorophylls (Chl) and carotenoids (Car) are major components of the photosynthetic apparatus. Under limiting irradiance conditions, the photosystems acquire a large Chl antenna size and the thylakoid membranes attain a low Chl *a*/Chl *b* ratio. Carotenoids participating in the so-called 'xanthophyll cycle' [3,4] are found in their epoxidized form with violaxanthin as the dominant species. Under high irradiance, especially under conditions when the absorbed light is greater than can be utilized by the photosynthetic apparatus, a number of chloroplast acclimation changes are elicited.

Abbreviations: Chl, chlorophyll; PS, photosystem; Q_A, primary electron accepting plastoquinone of photosystem II; LHC, light harvesting complex

* Corresponding author. Fax: +1-510-642-4995.
E-mail address: melis@nature.berkeley.edu (A. Melis).

0005-2728/01/$ – see front matter
PII: S0005-2728(01)00223-7

These include a smaller Chl antenna size for the photosystems, a higher Chl *a*/Chl *b* ratio in the thylakoid membrane (less Chl *b*), and conversion of violaxanthin (V) via antheraxanthin (A) to zeaxanthin (Z). Persistent irradiance stress brings about further, longer-term adjustments, including an increase in the pool size of the 'xanthophyll cycle' carotenoids.

Unicellular green algae are better suited to study acclimation responses of the photosynthetic apparatus than vascular plants, partly because they respond with a greater flexibility to the environment and partly because they display higher growth rates than crop or wild land plants. It has been shown that the Chl antenna size of unicellular green algae such as *Chlorella vulgaris* [5], *Chlamydomonas reinhardtii* [6,7], *Dunaliella tertiolecta* [8] and *Dunaliella salina* [9] becomes smaller in response to high irradiance. Overall, this is manifested as lower Chl content and higher Chl *a*/Chl *b* ratios in the high light (HL)-grown cells.

Prolonged exposure to strong irradiance impairs the photochemical efficiency of oxygenic photosynthesis. Photosystem (PS) II is the primary target of this inhibition, which is known as photoinhibition [10,11]. It is generally accepted that a photooxidative damage due to excess irradiance inhibits the function of the D1/32 kDa reaction center protein (*psbA* gene product) and stops photosynthesis. Reactive oxygen species generated at PSII, e.g. singlet oxygen, are thought to play a primary role in this adverse effect, one that entails irreversible chemical modification of the PSII reaction center Chl, P680 [10–12]. Restoration of PSII function following such photooxidative damage requires the removal–degradation of the inactive D1, and replacement by a de novo synthesized protein in the PSII holocomplex [10,11].

Numerous Chl-deficient mutants of vascular plants have been isolated and characterized to date. In general, these phenotypes show an amplified response to irradiance stress [13–15], including a reduction in the Chl antenna size and light harvesting complex (LHC) protein content, and accumulation of the xanthophyll cycle carotenoids [13,16]. Several such yellow–green Chl-deficient mutants of higher plants have been characterized in detail [13,14,17–23]. However, little or no comparable information is available on green algae [24,25]. Moreover, although cyanobacterial and green algal mutants have been used extensively to study the biogenesis and function of photosynthetic complexes [26–28], so far only a handful of mutants from the genus *Dunaliella* have been reported [29]. Photosynthesis mutants of the commercially important green alga *D. salina* have yet to be described in the literature. In this study, a yellow–green mutant of *D. salina* (henceforth denoted as (*dcd*1), exhibiting lower levels of total Chl, an elevated Chl *a*/Chl *b* ratio, and diminished LHC proteins was isolated and characterized. The *dcd*1 mutant also showed enhanced susceptibility to photoinhibition, enhanced accumulation of the carotenoid biosynthesis-related (Cbr) protein [30,31] and of zeaxanthin, suggesting a cause-and-effect relationship between photoinhibition and Cbr-zeaxanthin. This novel green algal phenotype is discussed in terms of its enhanced sensitivity to irradiance stress and potential use in algal biotechnology for the generation of zeaxanthin, a high-value bioproduct.

2. Materials and methods

2.1. Cell growth conditions

The unicellular green alga *D. salina* Teod. [32] was grown photoautotrophically in hypersaline medium [33] in the presence of 25 mM $NaHCO_3$ as a supplemental inorganic carbon source. Cells were grown in flat 1 l bottles (3 cm optical path length) at 30°C under continuous illumination of 2000 μmol photons m^{-2} s^{-1} (high light) or 100 μmol photons m^{-2} s^{-1} (low light (LL)). Irradiance was measured with a LI-COR Model LI-185B radiometer. The cultures were shaken to ensure a uniform illumination of the cells. Cells were harvested when they were at a density of $2–2.5\times10^6$ cells ml^{-1}. Counting via a Neubauer ultraplane hemacytometer monitored cell density in the culture.

2.2. Mutagenesis and mutant selection

Transformation experiments with the *ble* gene as a selectable marker are well established for *C. reinhardtii* [34]. The *ble* gene has been developed as a dominant selectable marker for both prokaryotes and eukaryotes. The *ble* gene product binds to and neutralizes the antibiotic (zeocin), thus affording re-

sistance to this class of antibiotics. *D. salina* transformation using the *ble* plasmid as a dominant selectable marker was carried out as follows. Plasmid DNA (pSP124S) for transformation was linearized by *Bam*HI and then purified by agarose gel electrophoresis. LL wild-type *D. salina* were harvested by centrifugation on $1000\times g$ for 3 min and resuspended in 0.08 M NaCl medium containing *D. salina* at a cell density of 2×10^8 cells/ml. 0.3 mg glass beads (425–600 μm, Sigma), 0.3 ml of cell suspension, 0.1 ml of 20% PEG (8000) and 1 μg of linearized plasmid were added to a 10 ml culture tube. The mixture was vortexed for 30 s at maximum speed with a cyclomixer. Following this treatment, the algae were inoculated with 2 ml of 0.08 M NaCl containing *D. salina* medium then incubated overnight on a shaker under 50 μmol photons m^{-2} s^{-1}. To select for zeocin (Invitrogen, San Diego, CA, USA) tolerance, transformants were plated on a 1.5% agar plate containing 1 μg zeocin per ml. Twelve days after transformation, zeocin-resistant colonies were transferred to a microtiter well plate (96-well culture plate, Falcon, Franklin Lake, NJ, USA) containing low salt *D. salina* medium supplemented with zeocin (1 μg/ml). After incubation in the presence of the antibiotic for 10 days, cells were transferred to an agar plate (0.08 M NaCl containing *D. salina* medium without zeocin). A grid of independent colonies was assembled (48 colonies per petri plate). Two weeks after plating on a grid, the transformants were screened visually based on color appearance. Yellow or yellow–green colonies were selected for further analysis of pigment composition.

2.3. Pigment analysis

For pigment determination, cells or thylakoid membranes were extracted in 80% acetone and debris were removed by centrifugation at $10\,000\times g$ for 3 min. The absorbance of the supernatant was measured with a Shimadzu UV-160U spectrophotometer. The chlorophyll (*a* and *b*) concentration of the samples was determined according to Arnon [35], with equations corrected as in Melis et al. [36].

For HPLC analysis, a HPLC Hewlett Packard Series model 1100 equipped with a Waters Spherisorb S5 ODS1 4.6×250 mm Cartridge Column was used. Two milliliters of algal suspension were centrifuged in an Eppendorf centrifuge at 14 000 rpm for 2 min. The pigments were extracted from the algal cells upon addition to the pellet of 200 μl filtered 90% acetone and vortexing at maximum speed for 1 min. The extract was centrifuged in an Eppendorf centrifuge at 14 000 rpm and 15 μl of the filtered supernatant (0.2 μm nylon filter) were subjected to HPLC analysis. The pigments were separated using a solvent mixture of 0.1 M Tris–HCl pH 8.0 ddH_2O, acetonitrile, methanol and ethyl acetate. During the run, the solvent concentrations were 14% 0.1 M Tris–HCl, 84% acetonitrile and 2% methanol from 0 to 15 min. From 15 min to 19 min the solvent mixture consisted of 68% methanol and 32% acetonitrile. A post-run followed for 6 min with the initial solvent mixture. The flow rate was constant with 1.2 ml/min. Pigments were detected at $\lambda=445$ nm with a reference at $\lambda=550$ nm. Concentrations of individual pigments were determined from the HPLC profiles calibrated with standard samples of chlorophyll and carotenoid.

2.4. Thylakoid membrane isolation

Cells were harvested by centrifugation at $1000\times g$ for 3 min at 4°C. Samples were diluted with sonication buffer containing 100 mM Tris–HCl (pH 6.8), 100 mM NaCl, 5 mM $MgCl_2$, 0.2% polyvinylpyrrolidone 40, 0.2% sodium ascorbate, 1 mM aminocaproic acid, 1 mM aminobenzamidine and 100 μM phenylmethylsulfonyl fluoride (PMSF). Cells were broken by sonication in a Branson 200 Cell Disrupter operated at 4°C for 30 s (pulse mode, 50% duty cycle, output power 5). Unbroken cells and starch grains were removed by centrifugation at $3000\times g$ for 4 min at 4°C. The thylakoid membranes were collected by centrifugation of the supernatant at $75\,000\times g$ for 30 min at 4°C. The thylakoid membrane pellet was resuspended in a buffer containing 250 mM Tris–HCl (pH 6.8), 20% glycerol, 7% SDS and 2 M urea. Solubilization of thylakoid proteins was carried out for 30 min at room temperature. Samples were centrifuged in a microfuge for 5 min to remove unsolubilized material, β-mercaptoethanol was added to yield a final concentration of 10% and the samples were stored at −80°C.

2.5. SDS–PAGE and Western blot analysis

Samples were brought to room temperature prior to loading for electrophoresis and diluted accordingly to yield equal Chl concentrations. Gel lanes were loaded with an equal amount of Chl per lane. SDS–PAGE analysis was carried out according to Laemmli [37]. Gels were stained with 1% Coomassie brilliant blue R for protein visualization.

Electrophoretic transfer of the SDS–PAGE resolved proteins to nitrocellulose was carried out for 3–5 h at a constant current of 800 mA, in transfer buffer containing 50 mM Tris, 380 mM glycine (pH 8.5), 20% methanol and 1% SDS. Identification of thylakoid membrane proteins was accomplished with specific polyclonal antibodies raised in rabbit in this laboratory against the isolated reaction center D1 protein, the LHCII apoproteins, the *psaA*/*psaB* proteins (PSI) [38,39]. Anti-Cbr antibody was kindly provided by Dr. A. Zamir (Weizmann Institute of Science, Rehovot, Israel). Immunoreactive bands were detected either by ECL (enhanced chemiluminescence) employing horseradish peroxidase-conjugated secondary antibodies (Amersham Pharmacia Biotech, Piscataway, NJ, USA) or cross-reaction with the antibodies was detected by a chromogenic reaction with anti IgG secondary antibodies conjugated with alkaline phosphatase (Bio-Rad, Hercules, CA, USA). Immunoblots were scanned with a HP Scan Jet 5300C optical scanner connected to a MacIntosh/G3 computer. The NIH Image version 1.6 program was used for the deconvolution and quantitation of the bands.

2.6. RNA isolation and Northern blot analysis

Total RNA of *D. salina* was isolated with the RNeasy kit (Qiagen) according to the manufacturer's instructions. Then 10–20 μg of total RNA were separated on a denatured agarose gel (1%) and blotted onto a nylon membrane. RNA blots were hybridized with 1.3 kb *Eco*RI probe containing a cDNA of the *Lhcb* gene (pDT *cab*1 [40]). cDNA of chlorophyll *a* oxygenase (*CAO*) from *D. salina* was kindly provided by Prof. A. Tanaka (Institute of Low Temperature Science, Hokkaido University, Sapporo, Japan). Hybridizations were carried out at 65°C overnight and the membranes were washed twice with 2×SSC/0.1% at 65°C for 15 min, and twice with 0.2×SSC/0.1% at 65°C for 15 min, and exposed to an X-ray film. The relative amounts of *Lhcb* and *CAO* mRNA were estimated by densitometric scanning of the autoradiograms.

2.7. Chlorophyll fluorescence

The initial (F_0), variable (F_v) and maximum (F_{max}) chlorophyll fluorescence yield [41] of intact cells was measured upon excitation of the cultures with green light (CS 4-96 and CS 3-69 Corning Filters, actinic light intensity of 75 μmol photons m^{-2} s^{-1}). An aliquot from the culture was incubated in the dark for 10 min prior to the measurement and the chlorophyll fluorescence was recorded in the absence or presence of DCMU (2.5 μM final concentration).

2.8. Spectrophotometric analyses

For spectrophotometric measurements, the thylakoid membrane pellet was resuspended in a buffer containing 50 mM Tricine (pH 7.8), 10 mM NaCl, 5 mM $MgCl_2$. The amount of functional PSI and PSII reaction centers was estimated from the light *minus* dark absorbance difference measurements of P_{700} photooxidation and Q_A photoreduction, respectively [9,42]. The functional light harvesting Chl antenna size of PSI and PSII was measured from the kinetics of P_{700} photooxidation and Q_A photoreduction, respectively [42].

2.9. Oxygen evolution measurements

Oxygen evolution of the cultures was measured at 26°C with a Clark-type oxygen electrode illuminated with a slide projector lamp. Yellow actinic excitation was provided by a CS 3-69 Corning cutoff filter in combination with an Ealing 35-5453 VIQ5-8 filter. An aliquot of 5 ml cell suspension (2 μM Chl) was transferred to the oxygen electrode chamber. To ensure that oxygen evolution was not limited by the carbon source available to the cells, 100 μl of 0.5 M sodium bicarbonate solution (pH 7.4) were added to the suspension prior to the oxygen evolution measurements. The measurement of the light saturation curve of photosynthesis was implemented with the oxygen electrode, beginning with the registration of

dark respiration in the cell suspension, and followed by measurements of the rate of oxygen evolution at 30, 60, 125, 225, 330, 500, 750, 1100, 1300, 1800, 2220, and 3000 μmol photons m^{-2} s^{-1}. Registration and the rate (slope) of oxygen evolution at each light intensity step was recorded for about 2 min. The photon use efficiency of the cells was calculated from the initial slope of the light saturation curves of photosynthesis.

3. Results

3.1. Isolation of a D. salina chlorophyll-deficient (dcd1) mutant

Following transformation with the *ble* plasmid, about 5000 putative transformant colonies of *D. salina* were identified and screened. One mutant (*dcd*1) was selected on the basis of its yellow–green coloration. This mutant grew well in the presence of zeocin (1 μg/ml) and this phenotype has been stable in the absence of this antibiotic. Fig. 1 shows growth curves of wild-type and *dcd*1 mutant in a liquid medium under a light intensity of 100 μmol m^{-2} s^{-1} (LL), or 2000 μmol m^{-2} s^{-1} (HL). Wild-type and *dcd*1 mutant had similar growth rates under either LL or HL conditions. When grown in liquid medium, the mutant cells appeared pale green under LL while the wild-type was dark green. Under HL growth conditions, both wild-type and mutant turned yellow (Fig. 2). Cellular Chl content was lower in the mutant as compared to the wild-type under all growth conditions (Table 1). Under LL growth, cellular Chl content in the mutant was about 60% of that in the wild-type. The Chl content of both wild-type and *dcd*1 mutant declined with increasing growth irradiance. This effect [7] was more pronounced in the mutant compared to the wild-type. Thus, under HL growth, cellular Chl content in the mutant was about 40% of that in the wild-type (Table 1). Table 1 also shows that, when cultivated under LL, the Chl *a*/Chl *b* ratio of the mutant (9.9:1) was significantly higher than that of the wild-type (4.5:1). When cultivated under HL, the Chl *a*/Chl *b* ratio of wild-type cells was about 15:1 whereas the Chl *b* content of the mutant cells was below the detection level of the method employed, resulting in Chl *a*/Chl *b* ratios much higher than 20. Since Chl *b* is specifically associated with the light harvesting complex proteins, these results indicated a smaller Chl antenna size of the photosystems in the mutant than in the wild-type.

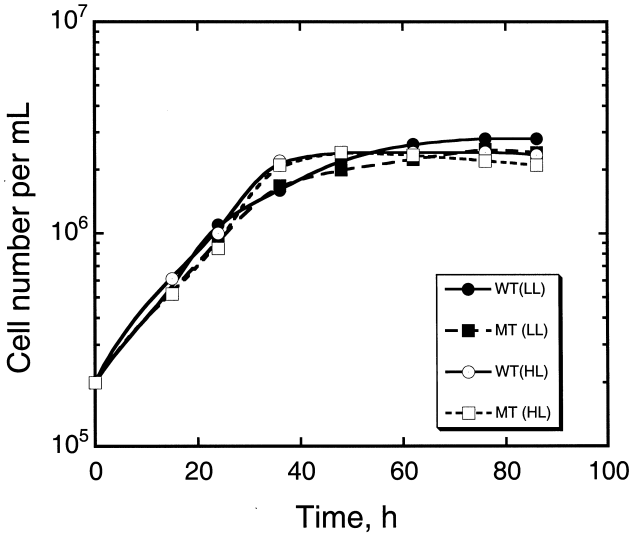

Fig. 1. Growth curves of *D. salina* wild-type and *dcd*1 mutant. Cell number is plotted as a function of time during growth. Cells were cultivated either under 100 μmol m^{-2} s^{-1} (LL) or 2000 μmol m^{-2} s^{-1} (HL).

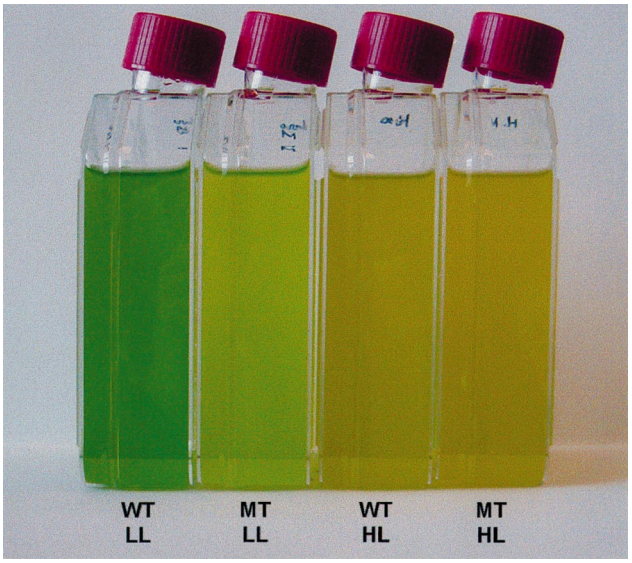

Fig. 2. Coloration of *D. salina* cultures in liquid medium. Wild-type (WT) and *dcd*1 mutant (MT) were grown either under low (100 μmol m^{-2} s^{-1}, LL) or high (2000 μmol m^{-2} s^{-1}, HL) irradiance.

Table 1
Photosynthetic apparatus parameters for *D. salina* wild-type and *dcd*1 mutant

Parameter	LL		HL	
	WT	MT	WT	MT
mol Chl $\times 10^{-15}$/cell	1.48 ± 0.21	0.85 ± 0.12	0.22 ± 0.01	0.1 ± 0.09
Chl *a*/Chl *b*	4.5 ± 0.1	9.9 ± 1.1	15 ± 2.2	> 20
mmol Q_A/cell	3.8×10^{-15}	2.5×10^{-15}	0.53×10^{-15}	0.29×10^{-15}
mmol P_{700}/cell	3.0×10^{-15}	2.28×10^{-15}	0.24×10^{-15}	0.16×10^{-15}
mmol Q_A/mol Chl	2.6 ± 0.07	3.0 ± 0.2	2.4 ± 0.16	2.9 ± 0.23
mmol P_{700}/mol Chl	2.1 ± 0.04	2.6 ± 0.4	1.09 ± 0.03	1.6 ± 0.06

Cells were grown under either 100 μmol m^{-2} s^{-1} (LL) or 2000 μmol m^{-2} s^{-1} (HL). Values represent means ± S.D. ($n = 3$–5).

3.2. Organization of the photosynthetic apparatus in wild-type and dcd1 mutant

In order to properly assess the photosynthetic apparatus organization in the thylakoid membrane of the *D. salina dcd*1 mutant, we determined the amounts of photochemically active Q_A and P_{700} spectrophotometrically. Quantitation of the functional PSII and PSI reaction centers was obtained from the light-induced absorbance change at 320 nm (Q_A) and 700 nm (P_{700}), respectively [43]. Table 1 presents the Q_A (PSII) and P_{700} (PSI) contents of the cells. The number of functional PSII and PSI reaction centers declined with irradiance in a manner that was qualitatively similar to that of Chl. Thus, regardless of the growth light intensity, on a per cell basis, the Q_A and P_{700} contents in the mutant were lower than those of the wild-type.

Measured on a per Chl basis, the Q_A and P_{700} contents of the mutant were higher than that of the wild-type, suggesting that the functional Chl antenna size of the mutant was smaller than that of the wild-type. Therefore, the effect of the mutation on the functional Chl antenna size of PSII and PSI was investigated in detail (see below).

3.3. Chlorophyll antenna size of the photosystems

The lower Chl content, the elevated Chl *a*/Chl *b* ratio and the higher per Chl Q_A and P_{700} contents in the mutant indicated a smaller Chl antenna size of the photosystems relative to that in the wild-type. Estimates of the functional Chl antenna size of PSI and PSII were obtained with the kinetic/spectrophotometric method [42,44]. In this approach, PSI and PSII are assigned functional Chl molecules in direct proportion to their respective rate of light absorption/utilization. Rates of light absorption/utilization for PSI and PSII were measured with isolated and DCMU poisoned thylakoids from the kinetics of P_{700} photooxidation and Q_A photoreduction, respectively [42]. Results, summarized in Table 2, show that thylakoid membranes of wild-type and *dcd*1 mutant contained two types of PSII, PSIIα and PSIIβ [45].

Table 2
Chlorophyll antenna sizes of PSII and PSI in *D. salina* wild-type and *dcd*1 mutant

Parameter	LL		HL	
	WT	MT	WT	MT
PSIIα	26 ± 7.4 (%)	24 ± 9.5(%)		
PSIIβ	74 ± 7.4 (%)	72 ± 9.5 (%)		
N-PSIIα	498 ± 31	411 ± 22		
N-PSIIβ	144 ± 5	127 ± 7		
N-PSII	236	190	44	39
N-PSI	181 ± 6	151 ± 15	122	95

The concentration of the various forms of PSII is given as the percentage of total PSII in the thylakoid membrane. The Chl antenna size of PSII and PSI is given as the number of Chl molecules functionally associated with each photosystem. Values given are the mean ± S.D.

The proportion of PSIIα and PSIIβ was similar in wild-type and *dcd*1 mutant. Further, Table 2 provides estimates for the functional Chl antenna sizes (*N*) of PSIIα, PSIIβ and PSI in the thylakoid membranes of wild-type and *dcd*1 mutant. In LL-grown wild-type cells, PSIIα contained about 498 ± 31 Chl (*a* and *b*) molecules whereas the Chl antenna size for PSIIα in the mutant (*N*-PSIIα = 411 ± 22) was significantly smaller. Wild-type PSIIβ contained about 144 ± 5 Chl molecules whereas mutant PSIIβ contained about 127 ± 5 Chl molecules. Overall, the average size of the PSII functional Chl antenna (defined from the statistical average of PSIIα and PSIIβ)

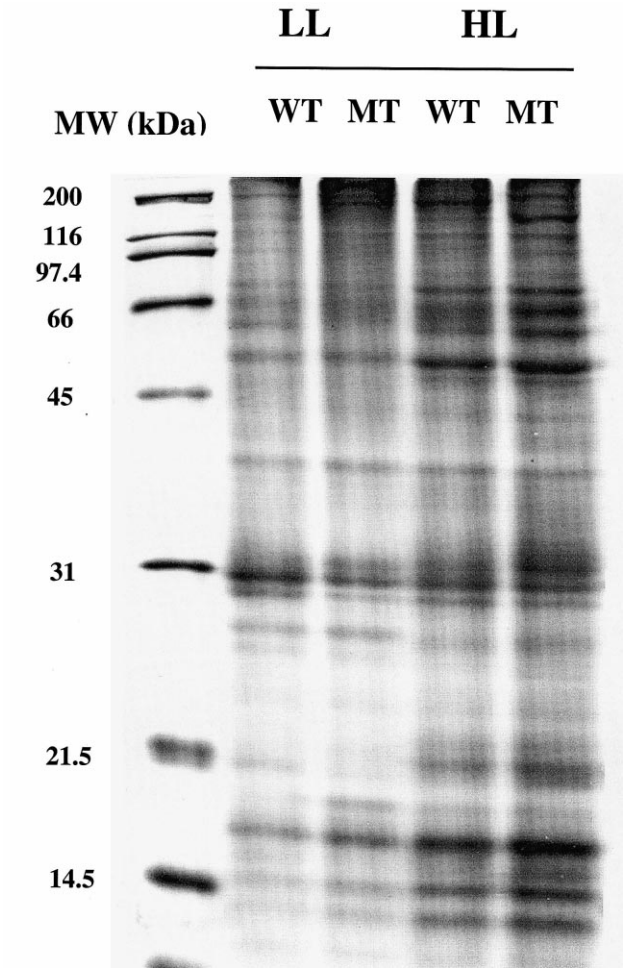

Fig. 3. SDS–PAGE profile of solubilized thylakoid membrane proteins from *D. salina* wild-type (WT) and *dcd*1 mutant (MT) cultivated under LL or HL growth conditions. Thylakoid membranes from these cells were isolated, solubilized and loaded at 4 nmol of Chl per lane.

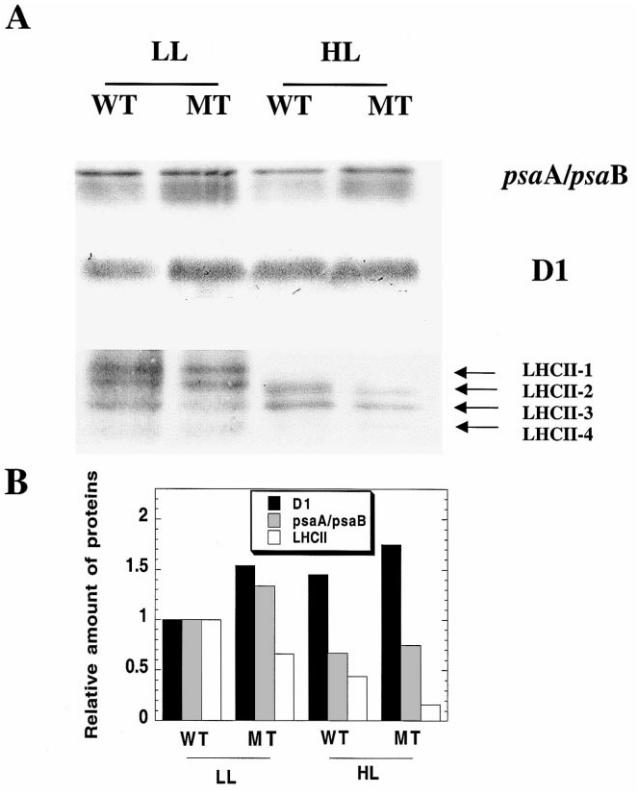

Fig. 4. Western blot analysis of electrophoretically separated thylakoid membrane proteins of *D. salina* wild-type (WT) and mutant (MT). Lanes were loaded on an equal Chl basis (4 nmol Chl per lane) and probed with specific polyclonal antibodies against the PSI *psaA*/*psaB* reaction center proteins, the PSII D1/32 kDa reaction center protein and the LHCII apoproteins. (B) Following a densitometric scan of the Western blots, estimated protein levels (D1, *psaA*/*psaB* and LHCII) of *D. salina* wild-type and mutant were quantified, normalized relative to the values of the WT-LL sample and plotted in a bar diagram.

was significantly smaller in LL-grown mutant cells (190 Chl molecules) as compared to the wild-type (236 Chl molecules). The PSI Chl antenna size of the mutant (*N*-PSI = 151 ± 15) was also smaller than that of wild-type (*N*-PSI = 181 ± 6).

In HL-grown *D. salina*, PSII did not display a Chl antenna size heterogeneity. The PSII Chl antenna size in wild-type contained 44 molecules whereas that of the mutant (*N*-PSII = 39) was slightly smaller. These Chl antenna size values are close to the minimum Chl antenna size of the PSII core, which is known to contain only about 37 Chl *a* molecules [46,47]. In HL-grown mutant cells, the PSI Chl antenna size (*N*-PSI = 95) was essentially that of the PSI core complex [46,47], whereas the Chl antenna size of

the wild-type contained 122 Chl molecules, i.e. it was significantly larger than the PSI core antenna.

3.4. Regulation of gene expression by irradiance in *D. salina*

Analysis of the functional Chl antenna size in the mutant already provided evidence for an altered photosynthetic apparatus organization. To further investigate alterations in protein composition of the photosystems in the mutant, thylakoid membranes were isolated from LL- and HL-grown cells. SDS–PAGE was performed with samples loaded on an equal Chl basis, followed by Western blot analysis with specific polyclonal antibodies. Fig. 3 shows the SDS–PAGE profile of thylakoid membrane proteins from wild-type and *dcd*1 mutant grown either under LL or HL conditions. Fig. 4 shows Western blot analyses of thylakoid membrane proteins isolated from wild-type and *dcd*1 mutant probed with specific polyclonal antibodies against the *psaA*/*psaB* reaction center proteins of PSI [48], the D1 reaction center protein of PSII [38], and the LHCII apoproteins [49].

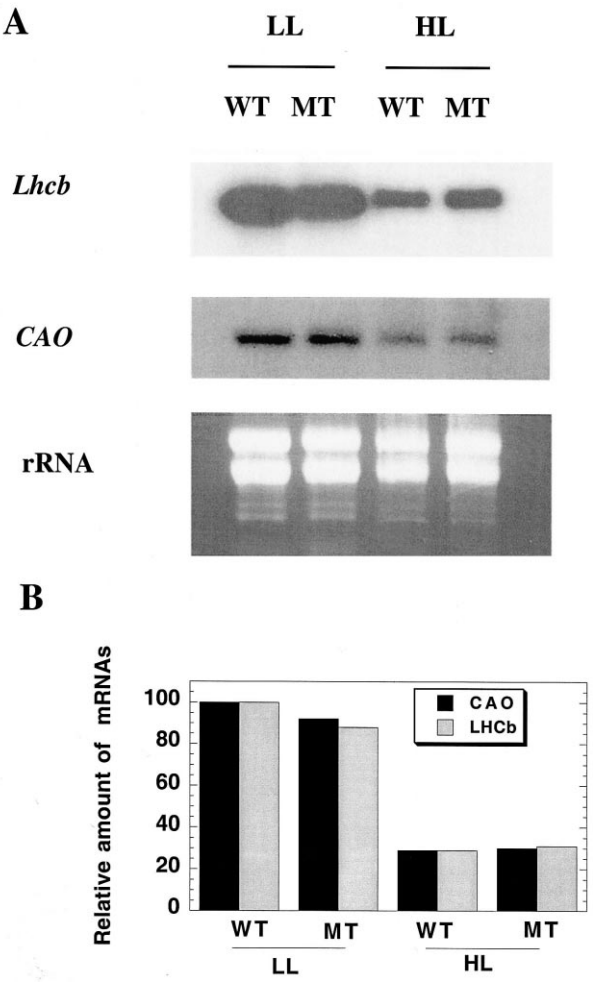

Fig. 5. Northern blot analysis of *Lhcb* and *CAO* gene transcripts from *D. salina* wild-type (WT) and *dcd*1 mutant (MT). (A) Autoradiogram of Northern blots and ethidium bromide-stained gel (to serve as a loading control). (B) Relative mRNA levels of *Lhcb* (light-shaded bars) and *CAO* (dark-shaded bars) of *D. salina* wild-type (WT) and mutant (MT) grown under LL and HL conditions. Quantified and normalized mRNA levels are shown relative to the LL-grown wild-type for each experiment. Relative densities are given as percent of the control.

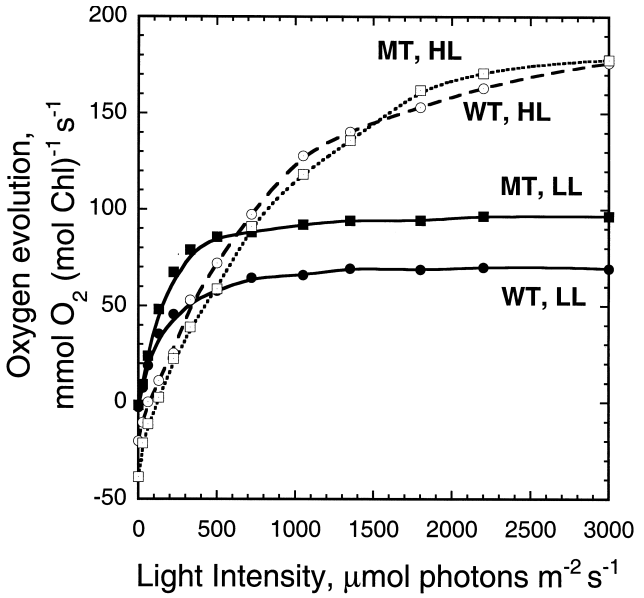

Fig. 6. The light saturation curves of photosynthesis in LL-grown wild-type (●), LL-grown mutant (■), HL-grown wild-type (○) and HL-grown mutant (□) *D. salina*. Rates of oxygen evolution on a per chlorophyll basis were measured as a function of actinic light intensity.

On a per Chl basis, and independent of growth irradiance, levels of *psaA*/*psaB* and D1 proteins were higher in the mutant than in the wild-type. This is consistent with the results of the spectrophotometric analysis (Table 1), in which the P_{700} and Q_A contents were greater in mutant than in the wild-type.

The amount and composition of the LHCII in wild-type and *dcd*1 mutant was estimated from Western blot analyses with specific polyclonal antibodies raised against the apoproteins of the LHCII (Fig. 4). In contrast to the reaction center proteins,

Table 3
Photosynthetic capacity, relative photon use efficiency and PSII photochemical efficiency in *D. salina* wild-type and *dcd*1 mutant

Parameter measured	LL		HL	
	WT	MT	WT	MT
Photon use efficiency (arbitrary units)	0.40	0.42	0.18	0.22
Photosynthetic capacity (P_{max}) (mmol O_2 (mol Chl)$^{-1}$ s^{-1})	70 ± 5.2	96.5 ± 1.2	170 ± 2.2	176 ± 1.7
F_v/F_{max}	0.6 ± 0.04	0.55 ± 0.02	0.28 ± 0.02	0.23 ± 0.04

Values shown represent the mean ± S.D.

the LHCII proteins of the mutant were greatly diminished relative to other membrane proteins regardless of the growth conditions. Four distinct bands of the LHCII (termed according to electrophoretic mobility as LHCII-1 through LHCII-4) were consistently present only in the LL-grown samples. In HL-grown samples, LHCII-1 was missing and the total level of the other LHCII apoproteins was significantly lower (Fig. 4, see also [49,50]). This response was more pronounced in the mutant than in the wild-type.

Given the significant alterations in photochemical apparatus organization, Chl *a*/Chl *b* ratio, light harvesting Chl antenna size and LHCII composition as a function of irradiance, we undertook to investigate the regulation of expression of the *Lhcb* gene. In addition, we studied the regulation of expression of the *CAO* gene [51], since formation of Chl *b* would be expected to be linked to LHC biosynthesis. *Lhcb* and *CAO* cDNAs were used as probes in Northern blot analyses of wild-type and *dcd*1 mutant grown under LL or HL conditions. The steady-state level of *Lhcb* transcripts from LL-grown wild-type and mutant was significantly greater than that of the HL-grown cells (Fig. 5A). This pattern was also observed when *CAO* transcripts were probed (Fig. 5A). However, there was no discernible difference in the level of transcripts between wild-type and mutant. It is evident that a significant down-regulation of *Lhcb* and *CAO* gene expression (Fig. 5B) occurred under HL stress in both wild-type and mutant. In sum, levels of *Lhcb* and *CAO* gene transcripts under HL growth were only about 25% of those measured under LL growth conditions. We determined that, on a per cell basis, *Lhcb* and *CAO* were attenuated in proportion to one another by irradiance (Fig. 5B), indicating coordinate regulation in the expression of these two genes.

3.5. *Efficiency and productivity of photosynthesis in D. salina*

The efficiency and productivity of photosynthesis in *D. salina* wild-type and *dcd*1 mutant were assessed upon comparative analysis of the light saturation curve of photosynthesis in the two strains. In such presentation, the rate of O_2 evolution was measured and plotted as a function of incident light intensity, thus obtaining the *photosynthesis* versus *irradiance* curve. From the slope of the initial linear part of the light saturation curve of photosynthesis, information was obtained about the relative photon efficiency of photosynthesis (Φ) in wild-type and mutant [52,53]. The light-saturated rate of oxygen evolution defined P_{max}, i.e. the capacity of photosynthesis, in the two strains [54]. Fig. 6 compares the light saturation curves of photosynthesis for wild-type and mutant grown under different light regimes. As shown in Table 3, LL-grown wild-type ($\Phi = 0.4$) and mutant ($\Phi = 0.42$) had similar photosynthetic efficiencies. However, when grown under HL conditions, photosynthetic efficiencies were less than half of the values measured for the corresponding LL-grown cells ($\Phi = 0.18$–0.22).

Under LL growth conditions, the photosynthetic capacity of the *dcd*1 mutant ($P_{max} = 96$ mmol O_2 (mol Chl)$^{-1}$ s^{-1}) was about 30% greater than that of the wild-type ($P_{max} = 70$ mmol O_2 (mol Chl)$^{-1}$ s^{-1}). In both LL-grown strains, photosynthesis was fully saturated at about 500 μmol photons m^{-2} s^{-1}. Under HL growth, the photosynthetic capacity of wild-type and mutant ($P_{max} = 180$ mmol O_2 (mol Chl)$^{-1}$ s^{-1}) was significantly greater than that measured under LL growth. Moreover, photosynthesis did not quite saturate even at 3000 μmol photons m^{-2} s^{-1}, a consequence of the substantially truncated Chl antenna size in the HL-grown strains [12].

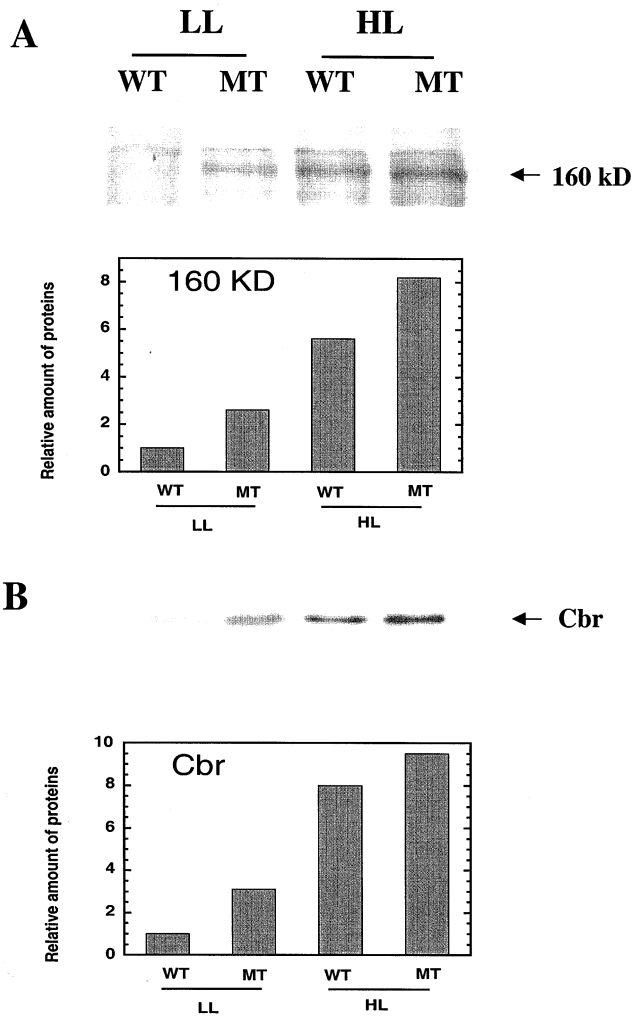

Fig. 7. (A) Western blot analysis of thylakoid membrane proteins of *D. salina* wild-type (WT) and mutant (MT), probed with specific polyclonal antibodies against the PSII D1/32 kDa reaction center protein, and densitometric quantitation of the level of the 160 kDa protein complex in the various samples. (B) Western blot analysis of thylakoid membrane proteins of *D. salina* wild-type (WT) and mutant (MT), probed with specific polyclonal antibodies against the Cbr protein, and densitometric quantitation of the level of the Cbr protein in the various samples. Lanes were loaded on an equal Chl basis (4 nmol Chl per lane).

Table 3 also compares the photochemical conversion efficiency of PSII determined from the F_v/F_{max} fluorescence ratio. Under LL growth conditions the PSII efficiency of the mutant ($F_v/F_{max} = 0.55$) was slightly lower than that of the wild-type ($F_v/F_{max} = 0.6$), suggesting a low-level photoinhibition in the mutant. The F_v/F_{max} ratios in wild-type and *dcd*1 mutant validate the similar photosynthetic efficiencies as measured from the light saturation curve of photosynthesis. PSII photochemical efficiency in the HL-grown cells was significantly lower ($F_v/F_{max} \approx 0.25$), suggesting significant photoinhibition of photosynthesis and accumulation of photodamaged PSII reaction centers in the thylakoid membrane of the two strains under HL conditions.

3.6. Photoinhibition of photosynthesis and zeaxanthin accumulation

Research from this laboratory has shown that the unicellular green alga *D. salina*, when exposed to long term photoinhibition conditions, responds by decreasing the Chl antenna size of PSI and PSII, by lowering the absolute amount of PSI in the chloroplast thylakoids, while maintaining relatively constant amounts of PSII. Under these conditions, however, a significant fraction of PSII was reported to occur as photochemically inactive centers [9,55]. Upon solubilization of such irradiance-stressed *D. salina* thylakoid membranes, photodamaged PSII reaction centers formed a cross-linked 160 kDa protein complex, which was readily distinguishable from the other thylakoid membrane proteins upon SDS–PAGE and Coomassie stain [38,56]. The 160 kDa complex contained a photodamaged but as yet undegraded D1 protein [38] as well as the D2 protein of the PSII reaction center [56]. This unusual property has permitted, for the first time, a SDS–PAGE-based quantitation of photodamaged versus active D1 in chloroplast thylakoids [57]. It was postulated that formation of such a 160 kDa complex might reflect PSII conformational changes that occur as a direct consequence of photodamage and the ensuing partial disassembly of PSII. The quantitative measurement of the 160 kDa complex provides a convenient way by which to assess the extent of in vivo photoinhibition in *D. salina*.

In the present study, we used this analytical approach to compare levels of photoinhibition in *D. salina* wild-type and *dcd*1 mutant. Fig. 7A shows the cross-reaction between PSII-specific polyclonal antibodies and a D1-containing protein band migrating to about 160 kDa. On a chlorophyll basis, very low levels of the 160 kDa protein were detected in LL-grown wild-type, consistent with the notion that

Table 4
Carotenoid composition in *D. salina* wild-type and *dcd*1 mutant

Parameter	N	V	A	Z	L	β-C	A+Z+V	(A+Z)/(A+Z+V)
WT (LL)	55 (2)	104 (2)	42 (4)	20 (2)	227 (10)	41 (4)	166	0.31
MT (LL)	40 (1)	123 (2)	77 (1)	47 (1)	235 (2)	68 (8)	247	0.51
WT (HL)	57 (8)	10 (1)	51 (10)	737 (65)	592 (9)	85 (15)	987	0.98
MT (HL)	46 (10)	16 (1)	155 (20)	2106 (230)	1068 (170)	127 (14)	2163	0.99

Whole-cell extracts were analyzed for pigment content. Cells were grown under either 100 μmol photons m^{-2} s^{-1} (LL) or 2000 μmol photons m^{-2} s^{-1} (HL). Carotenoid pigment data are presented on a chlorophyll basis (mmol Car per mol Chl). A, antheraxanthin; V, violaxanthin; N, neoxanthin; L, lutein; β-C, β-carotene. Values in parentheses show the S.D. of the measurement.

no photoinhibition is manifested under physiological irradiance conditions. Surprisingly, significant levels of this protein complex were detected in the thylakoid membrane of the mutant (MT) even under LL growth conditions (Fig. 7A, LL-MT). Mutant levels of the 160 kDa complex were about 2.5-fold greater than in the wild-type under these irradiance conditions. Under HL growth, levels of the 160 kDa complex were significantly greater in both strains with the mutant strain exhibiting about 50% higher level of the 160 kDa complex relative to the wild-type (WT) (Fig. 7A, HL).

Another indicator of irradiance stress in *D. salina* is accumulation of the Cbr protein [31,58]. The Cbr protein is a homologue to higher plant ELIPs and belongs to the LHC super family [59]. Thylakoid membrane proteins of LL- and HL-grown wild-type and *dcd*1 mutant cells were probed with a Cbr antibody (kindly provided by Dr. A. Zamir) and levels of the Cbr protein in wild-type and mutant were quantitated from Western blot analyses. Fig. 7B shows that the level of Cbr protein was about 3-fold higher in the LL-grown mutant than in the wild-type. As expected [60], Cbr levels were even higher in HL-grown *D. salina*. In this case, again, the mutant accumulated higher levels of the Cbr protein than the wild-type (Fig. 7B). Since the Cbr protein is generally thought to be an indicator of irradiance stress, these results are consistent with the notion of a greater susceptibility of the *D. salina* mutant strain to photooxidative stress and photoinhibition.

Yet another widely conserved irradiance stress response in green algae is the de-epoxidation state of xanthophylls in the photosynthetic apparatus [30,61–63]. The so-called 'xanthophyll cycle' [3] entails a reversible interconversion of Z, A and V, and has been shown to play a role in the non-photochemical quenching of excitation and the protection of the photosynthetic apparatus. Generally, cells accumulate violaxanthin and have low levels of Z under LL growth conditions whereas irradiance-stressed cells convert V to Z and accumulate the latter in the thylakoid membrane. This condition is designed to afford photoprotection to the photosynthetic apparatus under conditions of excess excitation [4,64].

To assess whether the *D. salina* mutant strain is subject to an enhanced de-epoxidation state relative to the wild-type, the carotenoid content of wild-type and *dcd*1 mutant were measured using HPLC. Table 4 shows a summary of this quantitative carotenoid analysis. On a per Chl basis, the LL-grown mutant contained 2.4-fold more Z than the wild-type. Overall, the xanthophyll pool size of the LL-grown mu-

Table 5
Total carotenoid (Car) and zeaxanthin (Z) content per dry mass weight in *D. salina* wild-type and *dcd*1 mutant

	LL		HL	
	WT	MT	WT	MT
Car/cell dw (mg/g)	10.2 ± 1.5	10.8 ± 1.1	8.24 ± 1.6	9.31 ± 1.6
Z/cell dw (mg/g)	0.43 ± 0.05	0.5 ± 0.02	2.8 ± 0.41	3.4 ± 0.39

Cells were grown under either 100 μmol m^{-2} s^{-1} (LL) or 2000 μmol m^{-2} s^{-1} (HL). Values represent means ± S.D. ($n = 3$–5).

tant was 1.5-fold greater than that of wild-type. Moreover, the de-epoxidation state of the xanthophyll pool size, represented by ((A+Z)/(A+Z+V)) was low (=0.31) in the wild-type but had an intermediate value in the mutant (=0.51). Growth under HL brought the epoxidation state of the xanthophyll pool close to unity, both in the wild-type and mutant (Table 4), a consequence of the nearly quantitative presence of zeaxanthin with only traces of violaxanthin detected in the photosynthetic apparatus of *D. salina* under these conditions. Table 5 presents an analysis of total carotenoid per cell dry weight (Car/cell dw) and zeaxanthin per cell dry weight (Z/cell dw) in wild-type and mutant grown under different irradiance conditions. It is seen that zeaxanthin, a commercially important xanthophyll, is slightly more abundant in the mutant than in the wild-type.

Fig. 8 further addresses changes in pigment ratios as *D. salina* cells acclimated to different light intensities. It is shown that the Z/Chl ratio in the wild-type changed from 0.02:1 in LL to 0.74:1 in HL. The change in the Z/Chl ratio in the wild-type appeared

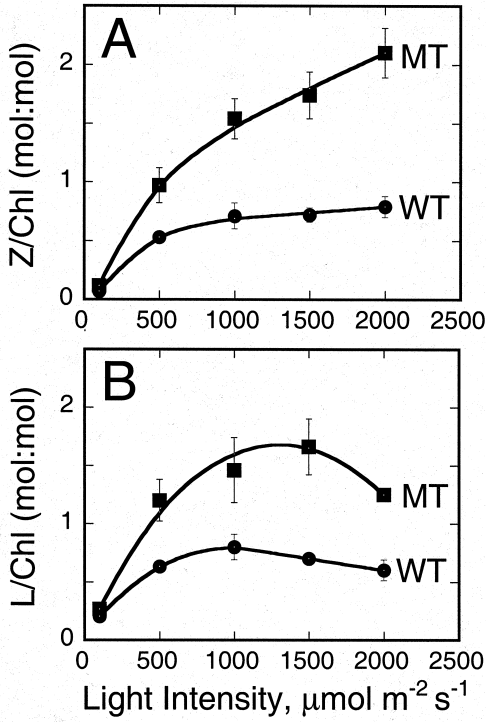

Fig. 8. Zeaxanthin (A) and lutein (B) per chlorophyll ratios in *D. salina* WT and MT grown at variable light intensities ranging from 100 to 2000 μmol photons m^{-2} s^{-1}.

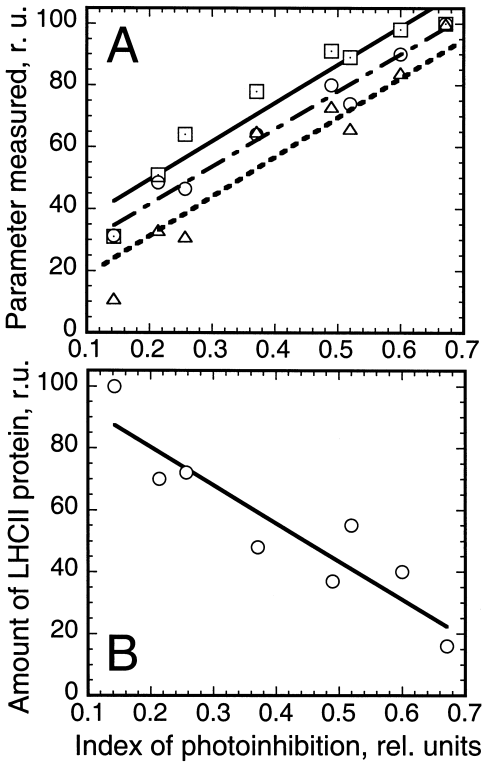

Fig. 9. (A) *D. salina* de-epoxidation state (□), relative amount of Cbr protein (△) and fraction of PSII existing as 160 kDa complexes (○) plotted as a function of the index of photoinhibition. The index of photoinhibition was derived from F_v/F_{max} ratio measurements, assuming limiting values of negligible photoinhibition when $F_v/F_{max}=0.7$ and maximal photoinhibition when $F_v/F_{max}=0$. Note the linear dependence of all three parameters on the index of photoinhibition. (B) Shown is the level of LHCII protein as a function of photoinhibition index. Note the linear decline in the level of the LHCII protein upon increasing photoinhibition.

to saturate at about 1000 μmol photons m^{-2} s^{-1} (Fig. 8A, WT). The Z/Chl ratio in the mutant changed from 0.047:1 in LL to 2.1:1, reached at 2000 μmol photons m^{-2} s^{-1}. Since Z accumulation is a response to irradiance stress, these results again suggested a greater sensitivity to irradiance stress for the mutant as compared to the wild-type. Qualitatively similar changes were measured for the lutein (L)/Chl ratio (Fig. 8B), although the amplitude of the lutein increase relative to Chl was not as pronounced as that of Z under HL conditions. Thus, the *dcd*1 mutant displays a greater zeaxanthin and lutein content and a lower chlorophyll content than the wild-type.

4. Discussion

Chlorophyll deficiency in photosynthetic organisms could be the result of a defect in the Chl biosynthetic pathway, resulting in diminished availability of Chl to the photosynthetic apparatus. Alternatively, a regulatory pathway may be activated under conditions when rates of light absorption exceed those that can be utilized by photosynthesis [1,2] causing a smaller Chl antenna size for the photosystems. Of interest is a class of mutants in which acclimation to irradiance is triggered at irradiance levels that are substantially lower than those activating the mechanism in the wild-type. These photoacclimation mutants have a smaller Chl antenna size of the photosystems under conditions when the corresponding wild-types are fully pigmented. This irradiance-dependent Chl antenna size decrease is disproportionately greater for PSII than for PSI resulting in alteration in photosystem stoichiometry [2,7]. Such mutants have been studied extensively among higher plants [16,19,20,23,65] but not among green algae.

A *D. salina* Chl-deficient yellow–green mutant (denoted here as *dcd*1) was isolated and studied in this work. Total chlorophyll content of the mutant was lower (by about 40%) than that of the wild-type, even under LL growth conditions. It displayed an elevated Chl *a*/Chl *b* ratio as well as a parallel lowering in the levels of Chl and LHCII apoprotein. In consequence, the Chl antenna size of the photosystems in the *dcd*1 mutant was significantly smaller than that of the wild-type. Unlike previously examined higher plant Chl-deficient mutants, the *dcd*1 was more susceptible to photoinhibition than its wild-type counterpart, onset of which appeared to occur at a much lower threshold of irradiance. Photoinhibition was manifested by a lowering of the F_v/F_{max} level and accumulation of a 160 kDa protein complex in the thylakoid membrane of *D. salina*. Concomitantly, and in parallel with an increase in these accepted markers of photoinhibition, *D. salina* wild-type and mutant showed a proportionately greater de-epoxidation state for the xanthophyll cycle carotenoids and enhanced levels of the Cbr protein.

In an effort to properly assess interrelationships among these photoacclimation responses, we undertook a comparative quantitative analysis of the changes measured. The various acclimation responses were normalized to the same maximum and plotted as a function of the extent of photoinhibition to the photosynthetic apparatus. The latter was estimated from the F_v/F_{max} ratio [66] in wild-type and *dcd*1 mutant grown under LL, ML (medium light) or HL conditions. In this analysis, we assumed that $F_v/F_{max} = 0.7$ reflects a steady-state situation with a minimal or negligible number of photodamaged PSII centers (index of photoinhibition = 0). Conversely, $F_v/F_{max} = 0.0$ corresponds to a quantitative accumulation of PSII reaction centers in the photodamaged state (index of photoinhibition = 1). Fig. 9A shows that zeaxanthin de-epoxidation state (Fig. 9A, squares), proportion of the 160 kDa photodamaged PSII complex (Fig. 9A, circles), and relative amount of the Cbr protein (Fig. 9A, triangles) all increase linearly as a function of photoinhibition index.

The strict quantitative correlation between xanthophyll de-epoxidation state, amount of Cbr protein and amount of the PSII repair intermediate (160 kDa complex) as a function of photoinhibition suggests a cause-and-effect relationship between these parameters. It is known that zeaxanthin acts as a quencher of excited Chl* molecules [67,68], thus, it is suggested that zeaxanthin plays a photoprotective role in PSII after photodamage and holocomplex disassembly have occurred. Such a view is consistent with recent observations in an obligate shade species in which the de-epoxidation state of the xanthophyll cycle carotenoids remained directly proportional to the level of photoinhibition in the leaves and independent of the light intensity seen by the plant [41,69,70]. Experimental evidence for the accumulation of zeaxanthin during photodamage, and possibly due to photodamage, was presented by Trebst et al. [71]. These observations raise the possibility that at least part of the zeaxanthin accumulation, which is induced upon photodamage to PSII, confers protection to the disassembled PSII from further and possibly irreversible photobleaching [69–72]. Photodamage is followed by a prompt disassembly of the PSII holocomplex [2,11,73] and it could be argued that this repair intermediate stage is when PSII is most vulnerable to massive and irreparable photooxidative bleaching. According to this scenario, zeaxanthin might play a pivotal role in the photoprotection of the photodamaged and disassembled PSII core, in-

cluding the D2, CP47 and CP43 Chl proteins. Thus, Cbr and zeaxanthin may be components of the PSII repair mechanism and may be critical for the protection of PSII as the latter is in the process of degrading and replacing non-functional D1 reaction center proteins. A return of zeaxanthin to violaxanthin, and a removal of the Cbr protein from the thylakoid membrane would logically follow the repair of PSII from photodamage and the recovery of the chloroplast from photoinhibition.

The Cbr protein was originally identified as a carotenoid biosynthesis-related protein, accumulating in green algae under irradiance stress and probably involved in the protection of the photosynthetic apparatus [31]. It is a homologue to the higher plant ELIP proteins (early light-induced proteins) and belongs to the LHC superfamily [59]. Previous structural analyses localized Cbr in the vicinity of the PSII core complex [30,31,74], consistent with a role for Cbr in photoprotection. These results served as the basis upon which to propose that Cbr protein may actually bind zeaxanthin [30,74]. Results in this work add new information to these earlier observations, showing a strict correlation between level of photodamage, amount of Cbr and xanthophyll de-epoxidation state in the thylakoid membrane of *D. salina*, suggesting a cause-and-effect relationship among these parameters. In this respect, the mutation in the *dcd*1 strain appears to have resulted in an increased susceptibility of the organism to photoinhibition. This is apparently manifested not only by the greater fraction of accumulated photodamaged PSII but also by the correspondingly elevated levels of Cbr and xanthophyll de-epoxidation state.

In contrast to the level of Cbr and xanthophyll de-epoxidation state, Fig. 9B shows a linear decrease in the level of LHCII protein as a function of photoinhibition index in the chloroplast thylakoids. This result shows the other facet of an integrated photoacclimation response and it clearly demonstrates the strong relationship between a number of regulatory parameters, including the down-regulation of the Chl antenna size of the photosystems upon irradiance stress. Down-regulation of Chl *b* and LHC occurs at least at the transcriptional level as evidenced by lower steady-state *CAO* and *Lhcb* mRNA levels (Fig. 5). This is consistent with recent results with higher plants [75] and green algae [76] showing that down-regulation of LHCII can occur at the transcriptional level. The data presented in this work are consistent with results of earlier reports showing that ELIPs are induced by stress conditions, such as photodamage, while LHCs are concomitantly down-regulated resulting in smaller Chl antenna size for the photosystems [75,77].

In spite of abundant physiological information, the underlying molecular mechanism for the regulation of the Chl antenna size is not well understood. Lower levels of Chl *b* and the smaller Chl antenna size in the *dcd*1 mutant, observed even under LL growth conditions, could be attributed to down-regulation of the *Lhcb* and *CAO* gene expression in the mutant as compared to the wild-type [53,78]. Alternatively, Chl deficiency and lower amounts of LHCII in the mutant may be attributed to diminished rates of Chl biosynthesis [79,80]. In any case, a lower Chl/cell and smaller Chl antenna size in the mutant, combined with a much higher Z/Chl and higher Z/cell could be an advantage in efforts to commercialize a green alga-based zeaxanthin production system. This is because a lower Chl/cell and smaller Chl antenna size in the mutant will permit higher photosynthetic solar conversion efficiencies and greater cell density in mass culture [12] while, at the same time, resulting in a greater content of zeaxanthin.

In summary, we presented evidence to show that Cbr protein accumulation and xanthophyll cycle de-epoxidation state are regulated in accordance to the extent of photodamage in the thylakoid membrane. These observations suggest involvement of zeaxanthin in the photoprotection of photodamaged and disassembled PSII core complexes. It could be argued that in the absence of a functional D1, these PSII core complexes could be subject to massive and irreversible photooxidative bleaching, a prospect mitigated by the presence of Cbr-zeaxanthin.

Acknowledgements

This work was supported by the ERC Program of the National Science Foundation under Award No. EEC-9731725. We thank Dr. A. Tanaka for making available the *D. salina CAO* cDNA, Dr. A. Zamir and Dr. I. Enami for providing anti-Cbr and anti-*psaA*/*psaB* specific polyclonal antibodies, respec-

tively, and Dr. K. Niyogi for making available HPLC equipment and for critical reading of the manuscripts.

References

[1] J.M. Anderson, Annu. Rev. Plant Physiol. 37 (1986) 93–136.
[2] A. Melis, Biochim. Biophys. Acta 1058 (1991) 87–106.
[3] H.Y. Yamamoto, Pure Appl. Chem. 51 (1979) 639–648.
[4] H.Y. Yamamoto, R. Bassi, in: D.R. Ort, C. Youcum (Eds.), Oxygenic Photosynthesis, Kluwer Academic Publishers, Dordrcht, 1996, pp. 539–563.
[5] A. Ley, D. Mauzerall, Biochim. Biophys. Acta 680 (1982) 95–106.
[6] P.J. Neale, A. Melis, J. Phycol. 22 (1986) 531–538.
[7] A. Melis, in: D.R. Ort, C.F. Yocum (Eds.), Advances in Photosynthesis. Vol. 4. Oxygenic Photosynthesis: the Light Reactions, Kluwer Academic Publishers, Dordrecht, 1996, pp. 523–538.
[8] A. Sukenik, J. Bennett, P.G. Falkowski, Biochim. Biophys. Acta 932 (1988) 206–215.
[9] B.M. Smith, P.J. Morrissey, J.E. Guenther, J.A. Nemson, M.A. Harrison, J.F. Allen, A. Melis, Plant Physiol. 93 (1990) 1433–1440.
[10] O. Prasil, N. Adir, I. Ohad (1992). in: J. Barber (Ed.), The Photosystems: Structure, Function and Molecular Biology, Elsevier Science, Amsterdam, 1992, pp. 295–342.
[11] E.M. Aro, I. Virgin, B. Andersson, Biochim. Biophys. Acta 1143 (1993) 113–134.
[12] A. Melis, J. Neidhardt, J.R. Benemann, J. Appl. Phycol. 10 (1999) 515–525.
[13] W.G. Hopkins, J.B. German, D.B. Hayden, Z. Pflanzenphysiol. 100 (1980) 15–24.
[14] W.G. Hopkins, D.B. Hayden, M.G. Neuffer, Z. Pflanzenphysiol. 99 (1980) 417–426.
[15] J.F. Allen, A. Melis, Biochim. Biophys. Acta 933 (1988) 95–106.
[16] T.G. Falbel, L. Staehlin, W. Adams III, Photosynth. Res. 42 (1994) 191–202.
[17] C.L. Rhyn, Genetics 40 (1954) 235–245.
[18] G.R. Stringam, Can. J. Genet. Cytol. 20 (1978) 329–336.
[19] A. Melis, A. Thielen, Biochim. Biophys. Acta 589 (1980) 275–286.
[20] A. Thielen, H. Van Gorkom, Biochim. Biophys. Acta 635 (1981) 111–120.
[21] M.L. Polacco, D.B. Walden, J. Hered. 78 (1987) 81–86.
[22] B. Greene, D. Allred, D. Morishige, L. Staehelin, Plant Physiol. 87 (1988) 357–364.
[23] B. Greene, L. Staehelin, A. Melis, Plant Physiol. 87 (1988) 350–356.
[24] R. Sager, Genetics 40 (1955) 476–489.
[25] I. Gyurjan, N.P. Yurina, M.S. Turischeva, M.S. Odintsova, N.N. Alexandrova, Planta 147 (1980) 287–294.
[26] M. Hippler, K. Redding, J.-D. Rochaix, Biochim. Biophys. Acta 1367 (1998) 1–62.
[27] J. Sun, A. Ke, P. Jin, V.P. Chitnis, P.R. Chitnis, Methods Enzymol. 297 (1998) 124–139.
[28] Z. Sun, F.X. Cunningham, E. Gantt, Proc. Natl. Acad. Sci. USA 95 (1998) 11482–11488.
[29] A. Shaish A, A. Ben-Amotz, M. Avorn, J. Phycol. 27 (1991) 652–656.
[30] H. Levy, T. Tal, A. Shaish, A. Zamir, J. Biol. Chem. 268 (1993) 20892–20896.
[31] A. Lers, H. Levy, A. Zamir, J. Biol. Chem. 266 (1991) 13698–13705.
[32] R.C. Starr, J. Phycol. 14 (1978) 47–100.
[33] U. Pick, L. Karni, M. Avron, Plant Physiol. 81 (1986) 92–96.
[34] V. Lumbreras, D.R. Stevens, S. Purton, Plant J. 14 (1998) 441–448.
[35] D.I. Arnon, Plant Physiol. 24 (1949) 1–15.
[36] A. Melis, M. Spangfort, B. Andersson, Photochem. Photobiol. 45 (1987) 129–136.
[37] U.K. Laemmli, Nature 227 (1970) 680–685.
[38] J.H. Kim, J.A. Nemson, A. Melis, Plant Physiol. 103 (1993) 181–189.
[39] M.A. Harrison, A. Melis, Plant Cell Physiol. 33 (1992) 627–637.
[40] J. LaRoche, J. Bennett, P.G. Falkowski, Gene 95 (1990) 165–172.
[41] C.C. Xu, H.-Y. Lee, C.-H. Lee, J. Plant Physiol. 155 (1999) 755–761.
[42] A. Melis, Philos. Trans. R. Soc. London Ser. B Biol. Sci. 323 (1989) 397–409.
[43] A. Melis, J.S. Brown, Proc. Natl. Acad. Sci. USA 77 (1980) 4712–4716.
[44] A. Melis, J.M. Anderson, Biochim. Biophys. Acta 724 (1983) 473–484.
[45] A. Melis, L.M.N. Duysens, Photochem. Photobiol. 29 (1979) 373–382.
[46] A. Manodori, M. Alhadeff, A.N. Glazer, A. Melis, Arch. Microbiol. 139 (1984) 117–123.
[47] R.E. Glick, A. Melis, Biochim. Biophys. Acta 934 (1988) 151–155.
[48] Y. Kashino, I. Enami, K. Satoh, S. Katoh, Plant Cell Physiol. 31 (1990) 479–488.
[49] A. Tanaka, A. Melis, Plant Cell Physiol. 38 (1997) 17–24.
[50] M.R. Webb, A. Melis, Plant Physiol. 107 (1995) 885–893.
[51] A. Tanaka, H. Ito, R. Tanaka, N.K. Tanaka, K. Yoshida, K. Okada, Proc. Natl. Acad. Sci. USA 95 (1998) 12719–12723.
[52] O. Bjorkman, B. Demmig, Planta 170 (1987) 489–504.
[53] P.J. Neale, J.J. Cullen, M.P. Lesser, A. Melis, in: H.Y. Yamamoto, C.M. Smith (Eds.), Photosynthetic Responses to the Environment. Current Topics in Plant Physiology, American Society of Plant Physiologists Publ. Ser. 8, 1993, pp. 61–77.
[54] S.B. Powles, C. Critchley, Plant Physiol. 65 (1980) 1181–1187.

[55] C. Vasilikiotis, A. Melis, Proc. Natl. Acad. Sci. USA 91 (1994) 7222–7226.
[56] A. Melis, J.A. Nemson, Photosynth. Res. 46 (1995) 207–211.
[57] I. Baroli, A. Melis, Planta 198 (1996) 640–646.
[58] H. Levy, I. Gokhman, A. Zamir, J. Biol. Chem. 267 (1992) 18831–18836.
[59] B.R. Green, W. Kuehlbrandt, Photosynth. Res. 44 (1995) 139–148.
[60] E. Andreasson, A. Melis, Plant Cell Physiol. 36 (1995) 1483–1492.
[61] K.K. Niyogi, Annu. Rev. Plant Physiol. Plant Mol. Biol. 50 (1999) 333–359.
[62] D.P. Maxwell, F. Stefan, N.P.A. Huner, Plant Physiol. 107 (1995) 687–694.
[63] M. Król, D.P. Maxwell, N.P.A. Huner, Plant Cell Physiol. 38 (1997) 213–216.
[64] B. Demmig-Adams, W.W. Adams III, B.A. Logan, A.S. Verhoeve, Aust. J. Plant Physiol. 22 (1995) 249–260.
[65] M.A. Harrison, J.A. Nemson, A. Melis, Photosynth. Res. 38 (1993) 141–151.
[66] W. Butler, M. Kitajima, Biochim. Biophys. Acta 376 (1976) 116–125.
[67] H.A. Frank, J.A. Bautista, J.S. Josue, A.J. Young, Biochemistry 39 (2000) 2831–2837.
[68] I. Baroli, K.K. Niyogi, Philos. Trans. R. Soc. London Ser. B Biol. Sci. 355 (2000) 1385–1394.
[69] B. Demmig-Adams, D.L. Moeller, A.L. Barry, W.W. Adams, Planta 205 (1998) 367–374.
[70] P. Jahns, B. Miehe, Planta 198 (1996) 202–210.
[71] B. Depka, P. Jahns, A. Trebst, FEBS Lett. 424 (1998) 267–270.
[72] P. Jahns, B. Depka, A. Trebst, Plant Physiol. Biochem. 38 (2000) 371–376.
[73] J.E. Guenther, A. Melis, Photosynth. Res. 23 (1990) 105–109.
[74] G. Banet, U. Pick, A. Zamir, Planta 210 (2000) 947–955.
[75] M. Heddad, I. Adamska, Proc. Natl. Acad. Sci. USA 97 (2000) 3741–3746.
[76] J. Escoubas, M. Lomas, J. LaRoche, P.G. Falkowski, Proc. Natl. Acad. Sci. USA 92 (1995) 10237–10241.
[77] M.H. Motané, K. Kloppstech, Gene 258 (2000) 1–8.
[78] C.E. Espineda, A.S. Linford, D. Devine, J.A. Brusslan, Proc. Natl. Acad. Sci. USA 96 (1999) 10507–10511.
[79] B. Dreyfuss, J. Thornber, Plant Physiol. 106 (1994) 829–839.
[80] T.G. Falbel, L.A. Staehelin, Physiol. Plant. 97 (1994) 311–320.